Journal of The Electrochemical Society, **157** (1) D50-D53 (2010)
0013-4651/2010/157(1)/D50/4/$28.00 © The Electrochemical Society

Electrodeposition of Ni–P Alloy–Multiwalled Carbon Nanotube Composite Films

Yosuke Suzuki,[a,*] Susumu Arai,[a,,z] and Morinobu Endo[b]**

[a]*Department of Chemistry and Material Engineering* [b]*Department of Electrical and Electronic Engineering, Faculty of Engineering, Shinshu University, Nagano 380-8553, Japan*

Ni–P alloy–multiwalled carbon nanotube (MWCNT) composite films were fabricated by an electrodeposition technique, and their microstructure, hardness, and frictional properties were analyzed. Ni–P alloy–MWCNT composite films containing 20–22 atom % P and 0.7–1.2 mass % MWCNTs were electrodeposited from a composite plating bath. MWCNTs were embedded relatively uniformly in the Ni–P alloy matrix. The hardness of the composite films was higher than that of the Ni–P alloy films, both before and after heat-treatment, and the friction coefficient of the composite films was lower than that of the Ni–P alloy films.
 [DOI: 10.1149/1.3254180]

Manuscript submitted May 20, 2009; revised manuscript received September 29, 2009. Published November 13, 2009.

Carbon nanotubes (CNTs)[1,2] have excellent mechanical characteristics, such as high tensile strength and high elastic modulus, as well as high thermal and electrical conductivity. Therefore, research into practical applications of CNTs, such as resin–CNT, ceramic–CNT, and metal–CNT composites, has been actively pursued.[3-5] Recently, the fabrication of metal–CNT composites has been attempted using an electrodeposition technique.[6,7] The present authors and others have also reported the fabrication and properties of electrodeposited metal–CNT composite films, such as Cu–CNT [8,9] and Ni–CNT.[10-12] However, fabrication of CNT composite films by an electroless plating technique has also been reported.[13-17] Li et al. reported the friction and wear behavior of Ni–P alloy–CNT composite coatings;[13] the wear resistance and friction coefficient of the composite coating were lower than those of the Ni–P coating. Yang et al. reported that the corrosion resistance of the Ni–P alloy–CNT composite coating was higher than that of the Ni–P coating.[14] Therefore, Ni–P alloy–CNT composite coatings are useful for practical applications, but no research on the fabrication of such coatings by electrodeposition has been reported. Electroless plating has several advantages over electrodeposition, such as the ability to produce a uniform film thickness and the capability of coating the insulator. Unfortunately, electroless plating also has several disadvantages, such as a chemically unstable plating bath and a relatively high temperature required to increase deposition speed. Coating mechanical components requires high productivity and low cost. So, we investigated the fabrication of Ni–P alloy–CNT composite coatings by electrodeposition.

In the present study, Ni–P alloy–multiwalled carbon nanotube (MWCNT) composite films were fabricated using an electrodeposition technique, and the microstructure and characteristics of the composite films were investigated. Commercially available MWCNTs were used without pretreatment.

Experimental

Commercially available (Showa Denko Co., Ltd.) vapor-grown MWCNTs were used in the present study, obtained via catalyst-assisted chemical vapor deposition and heat-treated at 2800°C in Ar for 30 min. The MWCNTs were typically 100–200 nm in diameter and 20 μm long. A Ni–P alloy plating bath (1 M $NiSO_4 \cdot 6H_2O$ + 0.2 M $NiCl_2 \cdot 6H_2O$ + 0.5 M H_3BO_3 + 1 M H_3PO_3 + 0.5 M $C_6H_5Na_3O_7$) was used as the base bath. The MWCNTs did not disperse uniformly in the base bath; therefore, homogeneous dispersion of 2–10 g dm^{-3} MWCNTs was obtained by the addition of 0.2–1.0 × 10^{-4} M polyacrylic acid (mean molecular weight of 5000; PA5000) as a dispersion agent to the base bath while stirring. Plating was performed at 50°C with aeration under galvanostatic conditions (current density: 5 A dm^{-2}; electric charge: 360 C cm^{-2}). A commercially available electrolytic cell (model I, Yamamoto-Ms Co., Ltd., 65 × 65 × 95 mm) was employed for electrodeposition. The volume of the plating bath was 250 cm^3. A pure copper plate (C1020P) and a stainless steel plate (SUS304) with an exposed surface area of 10 cm^2 (3 × 3.3 cm) were used as the substrates. A pure nickel plate was used as the anode. The phosphorus content was determined using an electron-probe microanalyzer (EPMA-1610, Shimadzu Seisakusho Co.). The MWCNT content of the composite films was directly weighed; thick Ni–P alloy–MWCNT composite films (>2 g) were prepared, and the nickel-alloy matrix of the composite films was subsequently dissolved in hot nitric acid. The MWCNTs in the nitric acid solution were then filtered, dried, and weighed. Heat-treatment of the deposits was performed using an IR heating furnace (minilamp annealer, MILA-3000, ULVAC-RIKO Inc.) at 400°C for 1 h under vacuum. A phase structure analysis of the deposits was performed using an X-ray diffractometer (XRD, XRD-6000, Shimadzu Seisakusho Co.). Surface morphology and cross-sectional texture were observed using a field-emission scanning electron microscope (JSM-7000F, JEOL). A cross-sectional polisher (SM-09010, JEOL) was used to prepare cross-section samples for observation. Hardness testing of the deposits was performed using a Vickers microhardness tester (DUH-201, Shimadzu Seisakusho Co.) on the cross-section samples. The friction properties of the films were measured using a ball-on-plate-type reciprocating friction abrasion test machine (MMS-2419, Nissho Denki Co.) with a 6.1 mm diameter alumina ball (Hv = 1500) as the countersurface. The reciprocating friction stroke was 8 mm, and the tests were conducted under a normal load of 2 N. The sliding speed was 0.5 mm s^{-1}, and the number of cycles was 50. All measurements were performed under ambient conditions without a lubricant.

Results and Discussion

Figure 1 shows the effect of the MWCNT concentration in the plating baths on the MWCNT content in the Ni–P alloy–MWCNT composite films. The phosphorus content of the films is also shown. The MWCNT content of the composite films increased with increasing MWCNT concentration in the plating baths and reached a maximum value of 1.19 mass %. However, the phosphorus content of the composite films was approximately constant at 20–25 atom %, regardless of the MWCNT concentration in the plating bath, although the phosphorus content of the Ni–P alloy–MWCNT composite films was slightly lower than that of the Ni–P alloy film. This was attributed to the adsorption of polyacrylic acid in the composite plating bath onto the cathode, which had affected the codeposition of phosphorus. In this investigation, the effect of varying phosphorus content in the deposited films (20–25 atom %) was assumed to be negligible.

Figure 2 shows the surface and cross-sectional SEM images of the Ni–P alloy–MWCNT composite films electrodeposited from

* Electrochemical Society Student Member.
** Electrochemical Society Active Member.
z E-mail: araisun@gipwc.shinshu-u.ac.jp

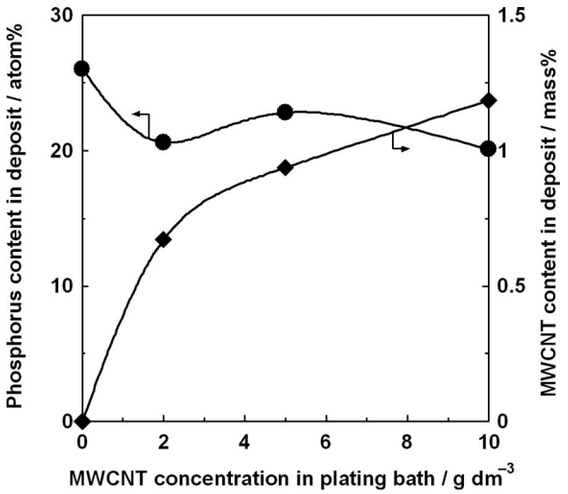

Figure 1. Variation in MWCNT content of the electrodeposited film and that of phosphorus content in the electrodeposited film with MWCNT concentration in the plating bath.

plating baths containing various concentrations of MWCNTs. The roughness and nonuniformity of the Ni–P alloy–MWCNT composite films increased with increasing MWCNT concentration. Large clusters of MWCNTs were observed on the surface of composite films electrodeposited from baths with higher concentrations of MWCNTs. These results show that the MWCNTs cohered and formed secondary particles in composite plating baths with MWCNT concentrations over 2 g dm^{-3}.

Figure 3 shows enlarged cross-sectional SEM images of the Ni–P alloy–0.7 mass % MWCNT composite film (the concentration of MWCNTs in the plating bath was 2 g dm^{-3}) before and after heat-treatment, where the black dots are cross sections of MWCNTs. No

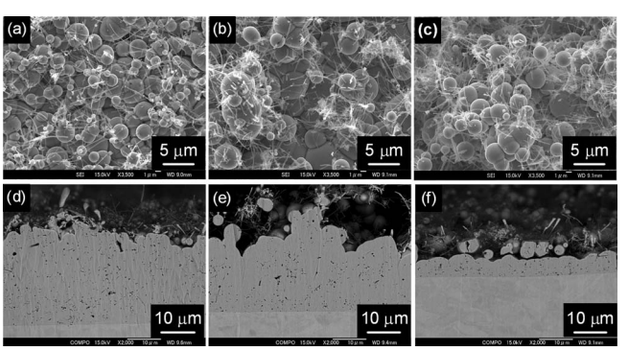

Figure 2. [(a)–(c)] Surface and [(d)–(f)] cross-sectional SEM images of the Ni–P alloy–MWCNT composite films. MWCNT concentration in the plating bath: (a) 2, (b) 5, (c) 10, (d) 2, (e) 5, and (f) 10 g dm^{-3}.

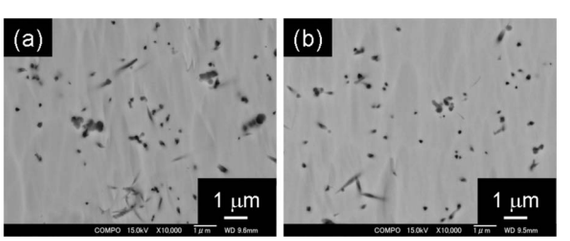

Figure 3. Cross-sectional SEM images of the Ni–P alloy–MWCNT composite film (a) before and (b) after heat-treatment. MWCNT concentration in the plating bath: 2 g dm^{-3}.

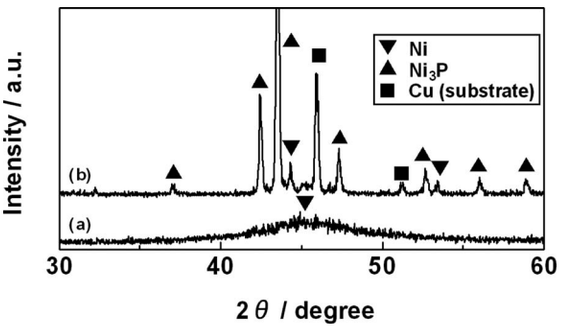

Figure 4. XRD patterns of the Ni–P alloy–MWCNT composite film (a) before and (b) after heat-treatment. MWCNT concentration in the plating bath: 2 g dm^{-3}.

change in microtexture was observed between the samples before and after heat-treatment. Voids and gaps between the Ni–P matrix and the MWCNTs were not observed in either SEM image.

Figure 4 shows the XRD patterns of the Ni–P alloy–MWCNT composite film before and after heat-treatment. Before heat-treatment, a broad peak assigned to nickel was observed at around 45°. After heat-treatment, the weak sharp peaks were assigned to nickel, and the strong sharp peaks were assigned to Ni_3P. According to the Ni–P binary alloy phase diagram, Ni–P alloys consist of face-centered cubic nickel and tetragonal Ni_3P in the phosphorus content range from 0 to 25 atom % at room temperature. Therefore, these results show that the metastable amorphous phase transformed to a stable crystalline phase.

Figure 5 shows the effect of the MWCNT content in the Ni–P alloy–MWCNT composite films on the hardness of the films before and after heat-treatment. The hardness of the Ni–P alloy film and the Ni–P alloy–MWCNT composite films was increased by heat-treatment. This increase in the hardness of the films can be attributed to the precipitation of the Ni_3P phase in the films.[18,19] Both before and after heat-treatment, the hardness of the Ni–P alloy–MWCNT composite films was higher than that of the Ni–P alloy film. These results agree with those reported by Yang et al.[14] and Wang et al.[15] This increase in hardness is believed to be caused by dispersion

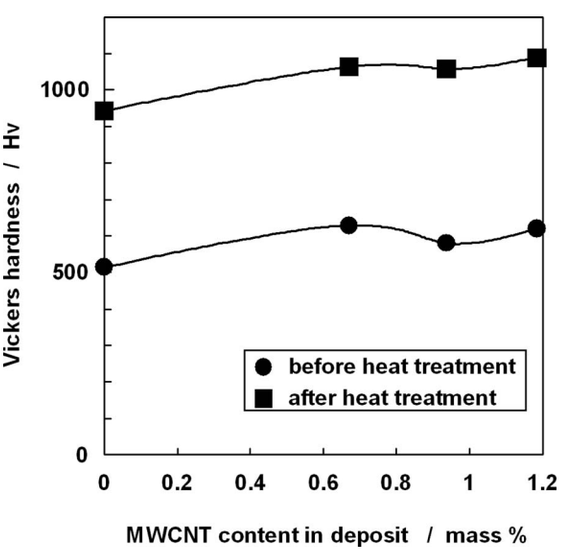

Figure 5. Hardness of the Ni–P alloy film and Ni–P alloy–MWCNT composite film before and after heat-treatment.

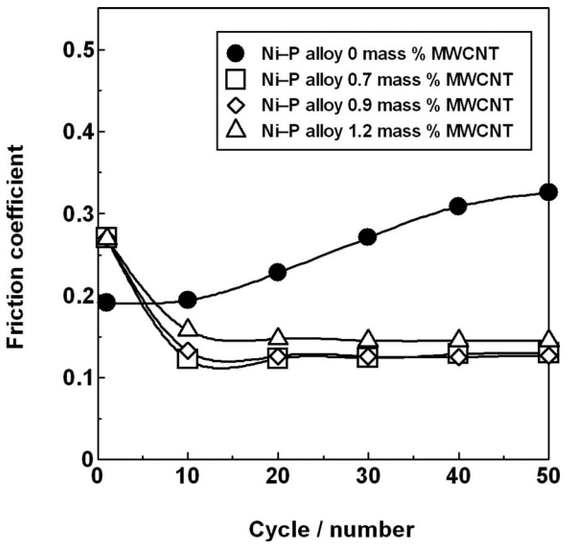

Figure 6. Relationship between the cycle number and the friction coefficient of the Ni–P alloy film and the Ni–P alloy–MWCNT composite film before heat treatment.

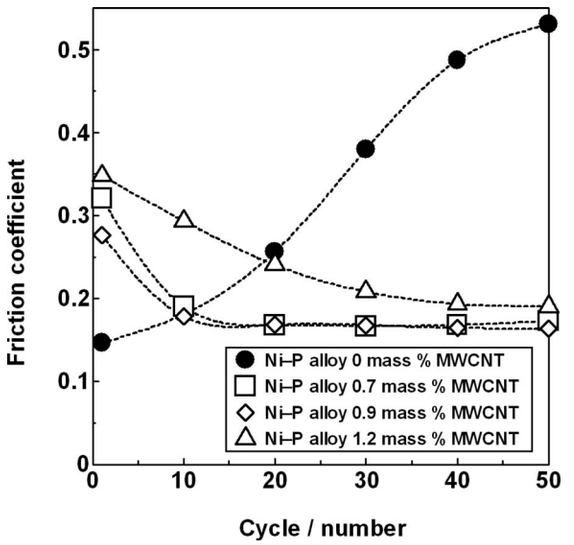

Figure 7. Relationship between the cycle number and the friction coefficient of the Ni–P alloy film and the Ni–P alloy–MWCNT composite film after heat-treatment.

hardening due to the MWCNTs. The hardnesses of the Ni–P alloy–MWCNT composite films remained approximately constant with increasing MWCNT content in the composite films.

Figure 6 shows the relationship between the cycle number and the friction coefficient of the Ni–P alloy and the Ni–P alloy–MWCNT composite films before heat-treatment. The friction coefficient of the Ni–P alloy film gradually increased with increasing cycle number. In contrast, the friction coefficient of the Ni–P alloy–MWCNT composite films decreased rapidly at an early stage and reached a steady value, indicating solid lubricity caused by the intrinsic solid lubricity of the MWCNTs.[20,21] The friction coefficient of the Ni–P alloy–1.2 mass % MWCNT composite film was higher than that of the Ni–P alloy–0.7 mass % MWCNT composite film and the Ni–P alloy–0.9 mass % MWCNT composite film. This trend is different from that of the paper by Chen et al. in that the friction coefficient decreased with increasing MWCNT content in the Ni–P MWCNT composite film.[22] The difference may be attributed to the large clusters of MWCNTs in the composite film. We intend to investigate this effect in detail soon.

Figure 7 shows the relationship between the cycle number and the friction coefficient of the Ni–P alloy film and the Ni–P alloy-MWCNT composite films after heat-treatment. Before heat-treatment, the friction coefficient of the Ni–P alloy film increased with increasing cycle number and that of the Ni–P alloy–MWCNT composite films gradually decreased and reached a steady value. Thus, the Ni–P alloy–MWCNT composite films exhibited solid lubricity even after heat-treatment. The friction coefficient of the Ni–P alloy–1.2 mass % MWCNT composite film was higher than that of the Ni–P alloy–0.7 mass % MWCNT composite film and the Ni–P alloy–0.9 mass % MWCNT composite film, as it was before heat-treatment. At 50 cycles, the friction coefficient of the Ni–P alloy–MWCNT composite film was approximately 0.1–0.2, both before and after heat-treatment. These results agree with papers on metal–MWCNT composite films.[12,15] This is because the friction coefficient of transversely aligned MWCNTs is about 0.1.[23]

Figure 8 shows the SEM images of worn surfaces of the Ni–P alloy and the Ni–P alloy–MWCNT composite films before and after heat-treatment. MWCNTs were observed on the worn surface of the Ni–P alloy-MWCNT composite film before and after heat treatment, which implies that the MWCNTs act as a solid lubricant.

Figure 9 schematizes the solid lubrication of the Ni–P alloy–MWCNT composite films.[12] The MWCNTs were arranged randomly on the surface of the Ni–P alloy–MWCNT composite film before the wear test (Fig. 9a). In this state, some of the MWCNTs may remain vertically arranged with respect to the alumina ball, and the friction coefficient may be high. In fact, the friction coefficient of the Ni–P alloy–MWCNT composite film was higher than that of Ni–P alloy film in the early stage (Fig. 6 and 7). Once the wear test begins, the alumina ball scratches the Ni–P alloy–MWCNT composite film, and the surface, especially the Ni–P alloy matrix, is gradually deformed plastically. Consequently, the MWCNTs are gradually repositioned transversely, resulting in a lower friction coefficient (Fig. 9b). Indeed, the friction coefficient of the Ni–P alloy–MWCNT composite film decreased with increasing number of cycles (Fig. 6 and 7).

Conclusions

Ni–P alloy–MWCNT composite films were fabricated by electrodeposition with MWCNTs homogeneously distributed throughout the Ni–P alloy matrix. The most homogeneous composite film was

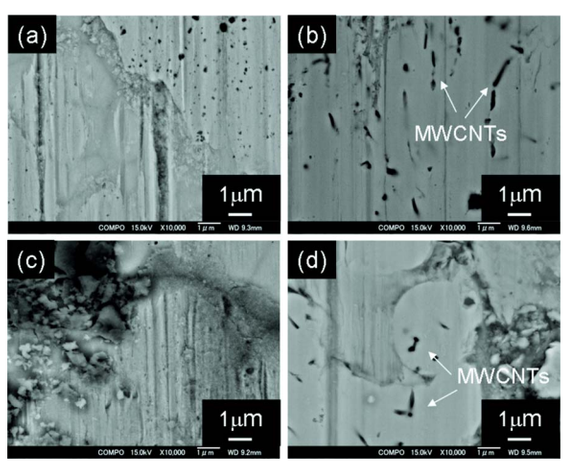

Figure 8. (Color online) SEM images of worn surfaces: Ni–P alloy film (a) before and (c) after heat-treatment and Ni–P alloy–MWCNT composite films (b) before and (d) after heat-treatment. MWCNT concentration in the plating bath is 2 g dm^{-3}.

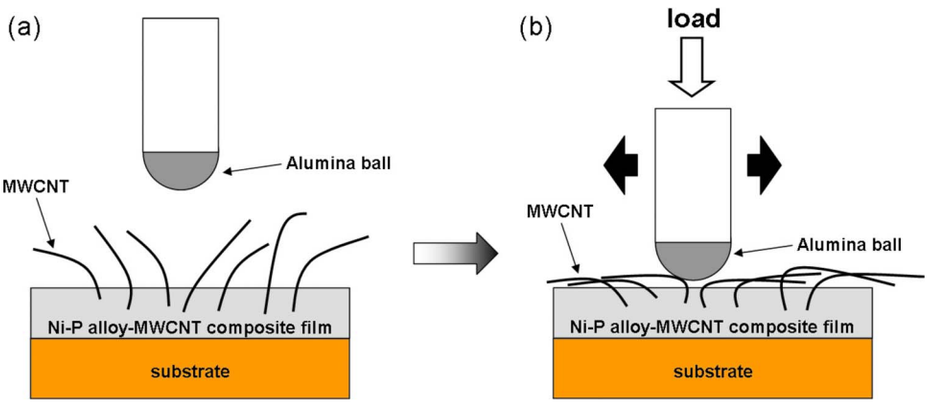

Figure 9. (Color online) A schematic illustration of the solid lubrication of a Ni–P alloy–MWCNT composite film (a) before the wear test and (b) during the wear test.

fabricated with an MWCNT concentration of 2 g dm^{-3} in the bath. The hardness of the composite film was higher than that of the Ni–P alloy film, both before and after heat-treatment. However, the hardness of the Ni–P alloy–MWCNT composite films remained approximately constant with increasing MWCNT content in the composite films. The friction coefficients of the composite films were lower than that of the Ni–P alloy film both before and after heat-treatment.

Acknowledgment

This research was supported by the CLUSTER (the second stage) of the Ministry of Education, Culture, Sports, Science and Technology of Japan.

Shinshu University assisted in meeting the publication costs of this article.

References

1. A. Oberlin, M. Endo, and T. Koyama, *J. Cryst. Growth*, **32**, 335 (1976).
2. S. Iijima, *Nature (London)*, **354**, 56 (1991).
3. Y. S. Zoo, J. W. An, D. P. Lim, and D. S. Lim, *Tribol. Lett.*, **16**, 305 (2004).
4. G. D. Zhan, J. D. Kuntz, J. L. Wan, and A. K. Mukherjee, *Nature Mater.*, **2**, 38 (2003).
5. J. Tan, T. Yu, B. Xu, and Q. Yao, *Tribol. Lett.*, **21**, 107 (2006).
6. Y. S. Jeon, J. Y. Byun, and T. S. Oh, *J. Phys. Chem. Solids*, **69**, 1391 (2008).
7. P. Q. Dai, W. C. Xu, and Q. Y. Huang, *Mater. Sci. Eng., A*, **483-484**, 172 (2008).
8. S. Arai and M. Endo, *Electrochem. Solid-State Lett.*, **7**, C25 (2004).
9. S. Arai and M. Endo, *Electrochem. Commun.*, **7**, 19 (2005).
10. S. Arai, M. Endo, T. Sato, and A. Koide, *Electrochem. Solid-State Lett.*, **9**, C131 (2006).
11. S. Arai, T. Saito, and M. Endo, *J. Electrochem. Soc.*, **154**, D530 (2007).
12. S. Arai, A. Fujimori, M. Murai, and M. Endo, *Mater. Lett.*, **62**, 3545 (2008).
13. Z. H. Li, X. Q. Wang, M. Wang, F. F. Wang, and H. L. Ge, *Tribol. Int.*, **39**, 953 (2006).
14. Z. Yang, H. Xu, Y. L. Shi, M. K. Li, Y. Huang, and H. L. Li, *Mater. Res. Bull.*, **40**, 1001 (2005).
15. L. Y. Wang, J. P. Tu, W. X. Chen, Y. C. Wang, X. K. Liu, C. Olk, D. H. Cheng, and X. B. Zhang, *Wear*, **254**, 1289 (2003).
16. W. X. Chen, J. P. Tu, H. Y. Gan, Z. D. Xu, Q. G. Wang, J. Y. Lee, Z. L. Liu, and X. B. Zhang, *Surf. Coat. Technol.*, **160**, 68 (2002).
17. W. X. Chen, J. P. Tu, Z. D. Xu, W. L. Chen, X. B. Zhang, and D. H. Cheng, *Mater. Lett.*, **57**, 1256 (2003).
18. K. H. Hou, M. C. Jeng, and M. D. Ger, *J. Alloys Compd.*, **437**, 289 (2007).
19. A. Bai and C. C. Hu, *Mater. Chem. Phys.*, **79**, 49 (2003).
20. W. X. Chen, F. Li, G. Han, J. B. Xia, L. Y. Wang, J. P. Tu, and Z. D. Xu, *Tribol. Lett.*, **15**, 275 (2003).
21. W. X. Chen, J. P. Tu, L. Y. Wang, H. Y. Gan, Z. D. Xu, and X. B. Zhang, *Carbon*, **41**, 215 (2003).
22. X. H. Chen, C. S. Chen, H. N. Xiao, H. B. Liu, L. P. Zhou, S. L. Li, and G. Zhang, *Tribol. Int.*, **39**, 22 (2006).
23. P. L. Dickrell, S. B. Sinnott, D. W. Hahn, N. R. Raravikar, L. S. Schadler, P. M. Ajayan, and W. G. Sawyer, *Tribol. Lett.*, **18**, 59 (2005).